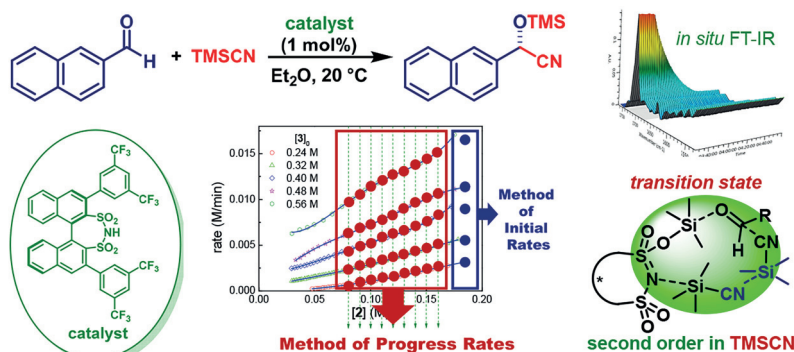# Kinetic Study of Disulfonimide-Catalyzed Cyanosilylation of Aldehydes by Using a Method of Progress Rates

Zhipeng Zhang [*a,b]
Martin Klussmann[b]
Benjamin List[b]

Abstract Kinetic study of organic reactions, especially multistep catalytic reactions, is crucial to in-depth understanding of reaction mechanisms. Here we report our kinetic study on the chiral disulfonimide-catalyzed cyanosilylation of an aldehyde, which revealed that two molecules of TMSCN are involved in the rate-determining C–C bond-forming step. In addition, the apparent activation energy, enthalpy of activation, and entropy of activation were deduced through a study of the temperature dependence of the reaction rates. More importantly, a novel and efficient method that makes use of the progress rates was developed to treat kinetic data obtained by continuous monitoring of the progress of a reaction by in situ FTIR.

Key words kinetics, progress rates, disulfonimides, cyanation, organocatalysis, aldehydes

Numerous novel catalysts and organic transformations are being developed nowadays, but mechanistic studies on these organic reactions, which would certainly facilitate a better understanding of the pathways and practical application of the reactions, have been left behind. Although theoretical studies have proved to be powerful in eliciting the mechanistic details of reactions,[1] experimental kinetic studies that provide details of the concentration dependence of the reactants and catalysts and which give rate and equilibrium constants of the reactions, thereby assisting in understanding the molecular-level behavior of the reaction, are still essential and irreplaceable in mechanistic studies.[2]

The catalytic asymmetric addition of cyanide to carbonyl compounds to give enantioenriched cyanohydrins is of great importance in organic synthesis, as chiral cyanohydrins are versatile synthetic intermediates for many biologically important compounds, such as α-hydroxy acids, α-

amino acids and β-amino alcohols. A large variety of catalysts, including enzymes,[3] metal-based Lewis acid catalysts,[4] organocatalysts,[5] and metal–organic frameworks,[6] have been developed in recent decades.[3–7] In 2016, List and co-workers reported efficient chiral disulfonimide organocatalysts **1a-H** and **1b-H** for the asymmetric cyanosilylation of aldehydes (Scheme 1) at catalyst loadings down to 50 ppm (0.005 mol%) with yields of up to 98%, enantiomeric ratios of up to 98:2, and reaction scales of up to 156 g.[8] Preliminary mechanistic investigations were conducted by in situ FTIR and NMR analysis, revealing that the catalytically active species is actually a silylated disulfonimide Lewis acid organocatalyst and that an interesting 'dormant period', induced mainly by water, precedes the real catalytic cycle, as every free hydroxy group (in water or the silanol) needs to be converted into the corresponding silyl ether before the actual cyanosilylation starts. Although these stud-
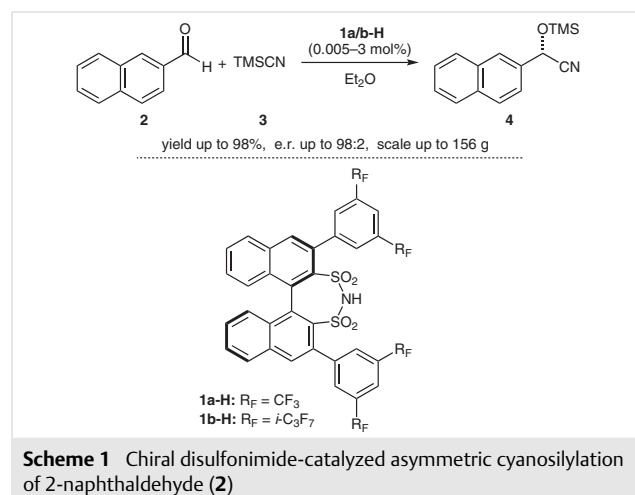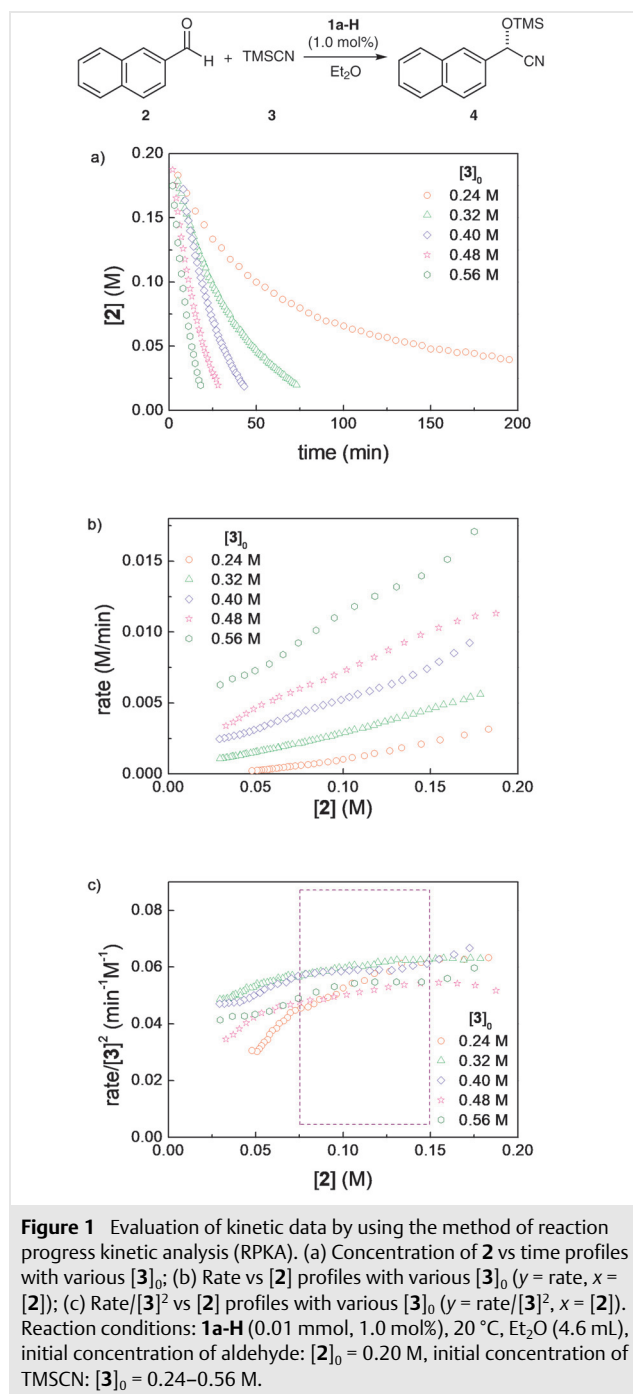

Scheme 1 Chiral disulfonimide-catalyzed asymmetric cyanosilylation of 2-naphthaldehyde (**2**)

ies provided a better understanding of the precatalytic cycle, details of the actual catalytic cycle remain unknown. Here, we report our detailed kinetic study on the cyanosilylation of 2-naphthaldehyde (**2**) catalyzed by disulfonimide **1a-H**, the results of which might contribute to an in-depth understanding of the reaction mechanism and to future development of new catalysts and transformations.

Experimental kinetic studies were carried out by monitoring the progress of the reaction by in situ FTIR [see Supporting Information (SI) for details]. To determine the reaction orders of all components, several reactions were carried out under identical conditions with various initial concentrations of reactants **2** and **3** and of catalyst **1a-H**. From the results of the in situ FTIR measurements, time profiles for the concentration of aldehyde [**2**] with various initial concentrations of TMSCN [**3**]$_0$ were obtained, as shown in Figure 1a. Profiles of [**2**] vs time with various initial concentrations of aldehyde [**2**]$_0$ and catalyst loadings [**1a-H**]$_0$ were also obtained (SI; Figures S13 and S16).

Reaction progress kinetic analysis (RPKA) is a method developed and formalized by Blackmond and co-workers.[9] Compared with the classical kinetic approach (method of pseudo-zero-order), where the concentration of one substrate is artificially fixed at a pseudo-constant high value (usually tenfold), RPKA permits reactions to be carried out under synthetically relevant conditions that are closer to standard reaction conditions and more reasonable. A key point of RPKA is to determine the reaction orders by a trial-and-error procedure by constructing graphical rate equations and attempting to find whether they overlay by dividing the rate curves by the concentration of the substrate under study raised to the power of the reaction order. We first evaluated our kinetic data by using the RPKA method.

Profiles for the concentration of aldehyde [**2**] vs time (Figure 1a) for various initial concentrations of TMSCN [**3**]$_0$ were converted into rate vs [**2**] profiles (Figure 1b) that clearly indicated a positive reaction order in [**3**], as the rate significantly increased upon increasing the concentration of **3**. The rate vs [**2**] profiles (Figure 1b) were then converted into rate/[**3**] vs [**2**] profiles (SI; Figure S8); however, no sign of an overlay between these graphical rate equations was observed. When the rate vs [**2**] profiles (Figure 1b) were further converted into rate/[**3**]^2 vs [**2**] profiles, as shown in Figure 1c, the graphical rate equations became much closer to each other, especially in the middle range of the reaction progress ([**2**] = 0.075–0.15 M). However, it was still difficult to judge whether these graphical rate equations overlaid one another or not. Although RPKA has proven to be a powerful method[2,9] for deducing reaction orders (mainly integer numbers such as 0 or 1) of the components participating in the reaction and for determining whether there is catalyst activation or deactivation and substrate or product inhibition or acceleration, it does not work as well when the reaction mechanism is more complex and the rate equation is more complicated (the orders can be nonintegers or even

Figure 1 Evaluation of kinetic data by using the method of reaction progress kinetic analysis (RPKA). (a) Concentration of **2** vs time profiles with various [**3**]$_0$; (b) Rate vs [**2**] profiles with various [**3**]$_0$ (y = rate, x = [**2**]); (c) Rate/[**3**]^2 vs [**2**] profiles with various [**3**]$_0$ (y = rate/[**3**]^2, x = [**2**]). Reaction conditions: **1a-H** (0.01 mmol, 1.0 mol%), 20 °C, Et$_2$O (4.6 mL), initial concentration of aldehyde: [**2**]$_0$ = 0.20 M, initial concentration of TMSCN: [**3**]$_0$ = 0.24–0.56 M.

negative if the overall rate expression for the reaction is written in power-law form). As mentioned by Blackmond,[9a] in some reactions, 'it may be found that none of the plots of graphical rate equations result in all the curves falling on top of one another.' In 2016, Burés developed a very simple and practical graphical method that uses a normalized time scale to determine the order in catalyst.[10a] However, this method is limited to the order in the catalyst concentration,

which is not a thermodynamic driving force of the reaction. Besides this quantity, the orders of the reactants also need to be determined in most kinetic studies. Later, Burés expanded his method and formalized the highly useful Variable Time Normalization Analysis (VTNA), which allows determining the order of any component of a reaction.[10b,c]

Seeking to make full use of the kinetic data obtained from the steady-state catalytic cycles of the entire reaction and to deduce the reaction orders of all components in a more efficient and convenient way, we developed a novel method for treating the kinetic data. Taking the determination of the order of TMSCN [3] as an example, the detailed procedures of this method are illustrated below (see SI for details).

Step 1. Obtain the rate vs [reactant A] profiles. Several reactions were carried out under identical conditions, varying only the initial concentration of reactant B, the order of which is to be determined [TMSCN (**3**) in this case]. The profiles of rate vs aldehyde concentration (Figure 1b; rate vs [**2**]) were obtained from the [**2**] vs time profiles, which were deduced from the data sets from the in situ FTIR measurements.

Step 2. Fit the rate vs [reactant A] profiles and get the functions. An accurate function (such as a high-order polynomial function) was used to fit the curves of each reaction in the rate vs [**2**] profiles (Figure 2a; blue lines).

Step 3. Obtain the data sets of (rate, [reactant B]). A series of concentrations of **2** (reactant A) with a fixed interval (in this case 0.01 M) and within a selected range (in this case 0.08–0.16 M) were used to calculate the instant progress rates from the fitting functions and the instant concentrations of **3** (reactant B) corresponding to each [**2**]. The obtained data sets of (rate, [**3**]) are shown as red squares in Figure 2a.

Step 4. Obtain the order of [reactant B] through a double log–arithmetic plot and by linear regression of the rate vs [reactant B] for each [reactant A]. A profile of the log(rate) vs log[**3**] was plotted for each [**2**] (Figure. 2b; [**2**] = 0.16 M). Linear regression of this profile gave a function whose slope corresponded to the order of [**3**] at this concentration of **2**. Thus, data sets of {(order of [**3**]), [**2**]} were obtained.

Step 5. Plot the profile of (order of [reactant B]) vs [reactant A]. The profile of (order of [**3**]) vs [**2**] was plotted (Figure 2c), which not only gave an approximate value for (order of [**3**]) but also indicated changes in the reaction order as a function of changing substrate concentrations.

This method might look complicated when described in steps, but all the fitting and data-processing steps can be easily done by using standard office software, such as *Microsoft Excel* and *Origin* (OriginLab Corp., Northampton, MA). The average value for the order of [**3**] was calculated to be 1.94 (nearly second order). Thus, the apparent rate order of **3** in the form of a power-law reaction rate equation was ob-

tained. The approximately second-order kinetics in TMSCN suggests that two molecules of this substrate are involved in a step that has a significant influence on the rate.

With the method described above, the average reaction order of aldehyde **2** was determined to be only 0.17, which is close to zero order. The average value for the order of cat-
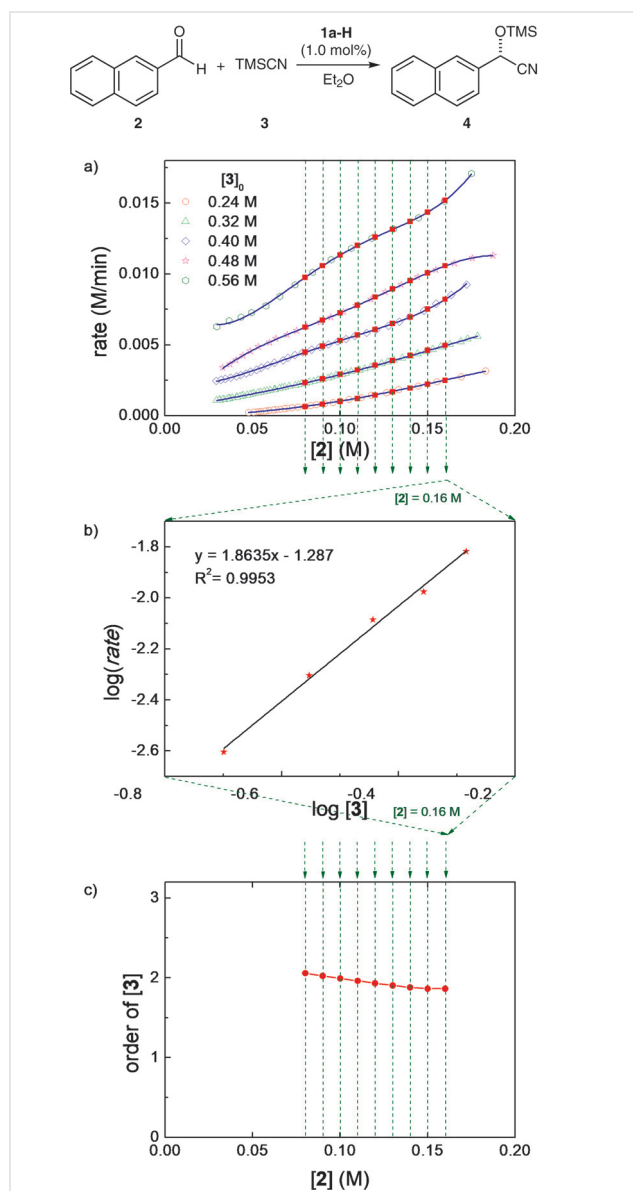

Figure 2 Determination of the order of TMSCN [**3**] by using a novel method that makes use of the progress rates: (2a) Rate vs [**2**] profiles with various initial concentration of **3** (fitted with high-order polynomial functions, shown as blue lines) and the resulting data sets of (rate, [**3**]) shown as red squares; (2b) Double logarithmic plot and linear regression of rate vs [**3**] when [**2**] = 0.16 M (the deduced order of [**3**] corresponds to the slope, 1.8635); (2c) The profile of (order of [**3**]) vs [**2**] in the selected range of [**2**] (0.08–0.16 M). *Reagents and conditions*: **1a-H** (0.01 mmol, 1.0 mol%), 20 °C, Et$_2$O (4.6 mL), initial concentration of aldehyde: [**2**]$_0$ = 0.20 M, initial concentration of TMSCN: [**3**]$_0$ = 0.24–0.56 M.
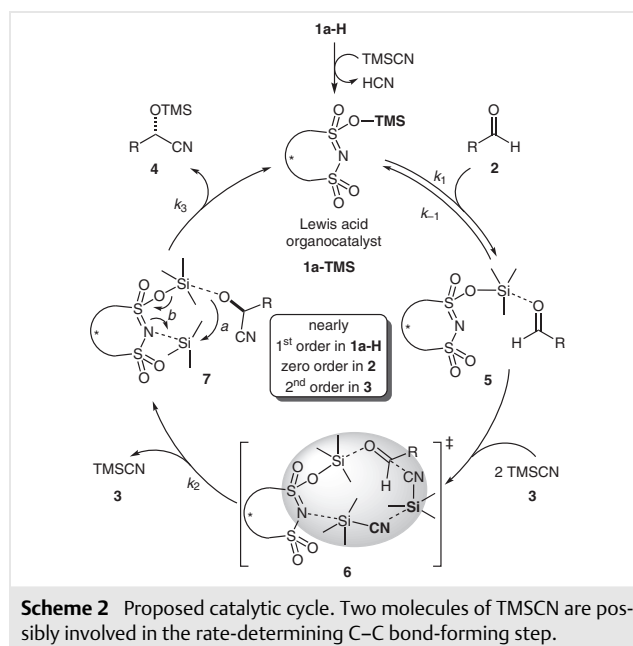
alyst **1a-H** was calculated to be 1.23 which is close to first order (see SI for details). Taking the average reaction orders determined by our method, the power-law form of the rate equation, which reflects the molecular-level behavior of the reaction as an empirical approximation, can be stated as shown in Equation 1. The low reaction order in **2** suggests that the step involving its activation is significantly faster than the addition of cyanide and that a catalyst species associated with aldehyde **2** is possibly involved in the rate-limiting step.

Rate = $k \cdot [\textbf{1a-H}]^{1.23} \cdot [\textbf{2}]^{0.17} \cdot [\textbf{3}]^{1.94}$ (Equation 1)

The temperature dependence of the reaction rates was studied in the range 273.15–303.15 K under otherwise identical conditions. The apparent activation energy of the reaction was deduced to be 41 kJ·mol^{-1} (9.9 kcal·mol^{-1}), according to the Arrhenius equation, by plotting $\ln(k)$ vs $1/T$ (SI; Figures S20 and S21); this implies that the reaction is relatively sensitive to temperature. The enthalpy of activation $\Delta H^{\ddagger}$ was deduced to be 39 kJ·mol^{-1} (9.3 kcal·mol^{-1}) and the entropy of activation $\Delta S^{\ddagger}$ was deduced to be –81 J·mol^{-1}·K^{-1} (–19 cal·mol^{-1}·K^{-1}) according to the Eyring equation by plotting $\ln(k/T)$ vs $1/T$. The Gibbs energy of activation $\Delta G^{\ddagger}$ was calculated to be 61 kJ·mol^{-1} (15 kcal·mol^{-1}) at 273.15 K (SI; Figures S22–S24).

On the basis of these studies, we propose the catalytic cycle for the disulfonimide-catalyzed asymmetric cyanosilylation of aldehydes shown in Scheme 2. After a long period of dormancy[8] of up to several hours, the precatalytic cycle ends. The Brønsted acid precatalyst **1a-H** then reacts with TMSCN to generate the catalytically active Lewis acid organocatalyst **1a-TMS** as a mixture of *O*- and *N*-silylated species.[8] This interacts with the aldehyde **2** to generate activated species **5**. The low reaction order in **2** suggests possible saturation kinetics in [**2**], indicating that the formation of **5** is significantly faster than the reverse reaction or the addition of cyanide. Subsequently, two molecules of TMSCN interact with **5**, possibly forming a new C–C bond through an aggregated cyclic transition state, as shown in **6**, to produce species **7** with regeneration of one molecule of TMSCN, which is proposed to be the rate-determining step. This is similar to the well-known Grignard reaction, which proceeds through an aggregated six-membered-ring transition state bridged by a dimeric dication of the Grignard reagent.[11] A study of the relationship between the enantiomeric excess of the product and the enantiomeric excess of the catalyst revealed that there is no nonlinear effect[12] in this reaction (SI; Figure S27), which is consistent with the involvement of a single catalyst molecule in the stereo-determining step. Finally, product **4** is quickly released from **7** and the active catalyst **1a-TMS** is regenerated.

In summary, a kinetic investigation of the disulfonimide-catalyzed cyanosilylation of an aldehyde was conducted and the orders of the reactants and catalyst for a power-law

Scheme 2 Proposed catalytic cycle. Two molecules of TMSCN are possibly involved in the rate-determining C–C bond-forming step.

form of the rate equation were obtained. An aggregated cyclic transition state involving two molecules of TMSCN was proposed. A novel and efficient method that makes use of the progress rates to deduce the orders for both reactants and catalyst was developed to treat kinetic data obtained from continuous monitoring of the progress of a reaction, and this is expected to attract widespread attention. We predict that these studies might not only facilitate an in-depth understanding of reaction mechanisms, but will also benefit the future design and application of powerful organocatalysts (for example, more-acidic chiral catalysts that could form aggregated cyclic transition states to increase reactivity and also enhance enantioselectivity in reactions of other silylated nucleophiles, such as silyl ketene acetals, enol silanes, TMSN$_3$ or TMSCF$_3$).[13]

Supporting Information

Supporting information for this article is available online at https://doi.org/10.1055/s-0040-1707129.

References

(1) Vogel, P.; Houk, K. N. In *Organic Chemistry: Theory, Reactivity, and Mechanisms in Modern Synthesis*; Wiley-VCH: Weinheim, **2019**.

(2) (a) Nishii, Y.; Ikeda, M.; Hayashi, Y.; Kawauchi, S.; Miura, M. *J. Am. Chem. Soc.* **2020**, *142*, 1621. (b) Romine, A. M.; Yang, K. S.; Karunananda, M. K.; Chen, J. S.; Engle, K. M. *ACS Catal.* **2019**, *9*, 7626. (c) Masson-Makdissi, J.; Jang, Y. J.; Prieto, L.; Taylor, M. S.; Lautens, M. *ACS Catal.* **2019**, *9*, 11808. (d) Shevick, S. L.; Obradors, C.; Shenvi, R. A. *J. Am. Chem. Soc.* **2018**, *140*, 12056. (e) Lee, C. F.; Diaz, D. B.; Holownia, A.; Kaldas, S. J.; Liew, S. K.; Garrett, G. E.; Dudding, T.; Yudin, A. K. *Nat. Chem.* **2018**, *10*, 1062. (f) Chung, R.; Vo, A.; Fokin, V. V.; Hein, J. E. *ACS Catal.* **2018**, *8*, 7889. (g) Wendlandt, A. E.; Vangal, P.; Jacobsen, E. N. *Nature* **2018**, *556*, 447. (h) Schreyer, L.; Kaib, P. S. J.; Wakchaure, V. N.; Obradors, C.; Properzi, R.; Lee, S.; List, B. *Science* **2018**, *362*, 216.

(3) (a) Effenberger, F. *Angew. Chem. Int. Ed.* **1994**, *33*, 1555. (b) Effenberger, F.; Förster, S.; Wajant, H. *Curr. Opin. Biotechnol.* **2000**, *11*, 532. (c) Gröger, H. *Adv. Synth. Catal.* **2001**, *343*, 547. (d) García-Urdiales, E.; Alfonso, I.; Gotor, V. *Chem. Rev.* **2005**, *105*, 313. (e) Sukumaran, J.; Hanefeld, U. *Chem. Soc. Rev.* **2005**, *34*, 530. (f) Holt, J.; Hanefeld, U. *Curr. Org. Synth.* **2009**, *6*, 15.

(4) (a) Zeng, X.-P.; Cao, Z.-Y.; Wang, X.; Chen, L.; Zhou, F.; Zhu, F.; Wang, C.-H.; Zhou, J. *J. Am. Chem. Soc.* **2016**, *138*, 416. (b) Laurell Nash, A.; Hertzberg, R.; Wen, Y.-Q.; Dahlgren, B.; Brinck, T.; Moberg, C. *Chem. Eur. J.* **2016**, *22*, 3821. (c) Wei, Y.-L.; Huang, W.-S.; Cui, Y.-M.; Yang, K.-F.; Xu, Z.; Xu, L.-W. *RSC Adv.* **2015**, *5*, 3098. (d) Lv, C.; Miao, C.-X.; Xu, D.; Wang, S.; Xia, C.; Sun, W. *Catal. Commun.* **2012**, *27*, 138. (e) Uemura, M.; Kurono, N.; Sakai, Y.; Ohkuma, T. *Adv. Synth. Catal.* **2012**, *354*, 2023. (f) Wen, Y. Q.; Ren, W. M.; Lu, X. B. *Chin. Chem. Lett.* **2011**, *22*, 1285. (g) Lv, C.; Cheng, Q.; Xu, D.; Wang, S.; Xia, C.; Sun, W. *Eur. J. Org. Chem.* **2011**, 3407. (h) Zhang, Z.; Wang, Z.; Zhang, R.; Ding, K. *Angew. Chem. Int. Ed.* **2010**, *49*, 6746. (i) North, M.; Omedes-Pujol, M.; Williamson, C. *Chem. Eur. J.* **2010**, *16*, 11367. (j) North, M.; Villuendas, P.; Williamson, C. *Tetrahedron* **2010**, *66*, 1915. (k) Belokon, Y. N.; Clegg, W.; Harrington, R. W.; Maleev, V. I.; North, M.; Pujol, M. O.; Usanov, D. L.; Young, C. *Chem. Eur. J.* **2009**, *15*, 2148. (l) Kurono, N.; Arai, K.; Uemura, M.; Ohkuma, T. *Angew. Chem. Int. Ed.* **2008**, *47*, 6643. (m) Zeng, B.; Zhou, X.; Liu, X.; Feng, X. *Tetrahedron* **2007**, *63*, 5129. (n) Liu, Y.; Liu, X.; Xin, J.; Feng, X. *Synlett* **2006**, 1085. (o) Lundgren, S.; Wingstrand, E.; Penhoat, M.; Moberg, C. *J. Am. Chem. Soc.* **2005**, *127*, 11592. (p) Hatano, M.; Ikeno, T.; Miyamoto, T.; Ishihara, K. *J. Am. Chem. Soc.* **2005**, *127*, 10776. (q) Liu, X.; Qin, B.; Zhou, X.; He, B.; Feng, X. *J. Am. Chem. Soc.* **2005**, *127*, 12224. (r) Belokon, Y. N.; Caveda-Cepas, S.; Green, B.; Ikonnikov, N. S.; Khrustalev, V. N.; Larichev, V. S.; Moscalenko, M. A.; North, M.; Orizu, C.; Tararov, V. I.; Tasinazzo, M.; Timofeeva, G. I.; Yashkina, L. V. *J. Am. Chem. Soc.* **1999**, *121*, 3968. (s) North, M.; Orizu, C.; Tararov, V. I.; Ikonnikov, N. S.; Belokon, Y. N.; Hibbs, D. E.; Hursthouse, M. B.; Abdul Malik, K. M. *Chem. Commun.* **1998**, 387. (t) Hamashima, Y.; Sawada, D.; Kanai, M.; Shibasaki, M. *J. Am. Chem. Soc.* **1999**, *121*, 2641. (u) Hamashima, Y.; Kanai, M.; Shibasaki, M. *J. Am. Chem. Soc.* **2000**, *122*, 7412.

(5) (a) Matsumoto, A.; Asano, K.; Matsubara, S. *Org. Lett.* **2019**, *21*, 2688. (b) Kurimoto, Y.; Nasu, T.; Fujii, Y.; Asano, K.; Matsubara, S. *Org. Lett.* **2019**, *21*, 2156. (c) Provencher, B. A.; Bartelson, K. J.; Liu, Y.; Foxman, B. M.; Deng, L. *Angew. Chem. Int. Ed.* **2011**, *50*, 10565. (d) Zuend, S. J.; Jacobsen, E. N. *J. Am. Chem. Soc.* **2007**, *129*, 15872. (e) Peng, D.; Zhou, H.; Liu, X.; Wang, L.; Chen, S.; Feng, X. *Synlett* **2007**, 2448. (f) Qin, B.; Liu, X.; Shi, J.; Zheng, K.; Zhao, H.; Feng, X. *J. Org. Chem.* **2007**, *72*, 2374. (g) Tian, S. K.; Deng, L. *Tetrahedron* **2006**, *62*, 11320. (h) Fuerst, D. E.; Jacobsen, E. N. *J. Am. Chem. Soc.* **2005**, *127*, 8964. (i) Ryu, D. H.; Corey, E. J. *J. Am. Chem. Soc.* **2005**, *127*, 5384. (j) Wen, Y.; Huang, X.; Huang, J.; Xiong, Y.; Qin, B.; Feng, X. *Synlett* **2005**, 2445. (k) Zhou, H.; Chen, F.-X.; Qin, B.; Feng, X.; Zhang, G. *Synlett* **2004**, 1077. (l) Li, Y.; He, B.; Feng, X.; Zhang, G. *Synlett* **2004**, 1598. (m) Ryu, D. H.; Corey, E. J. *J. Am. Chem. Soc.* **2004**, *126*, 8106. (n) Tian, S.-K.; Hong, R.; Deng, L. *J. Am. Chem. Soc.* **2003**, *125*, 9900. (o) Tian, S. K.; Deng, L. *J. Am. Chem. Soc.* **2001**, *123*, 6195. (p) Oku, J.; Ito, N.; Inoue, S. *Makromol. Chem.* **1979**, *180*, 1089.

(6) (a) Jin, F.-Z.; Zhao, C.-C.; Ma, H.-C.; Chen, G.-J.; Dong, Y.-B. *Inorg. Chem.* **2019**, *58*, 9253. (b) Li, Z.; Liu, Y.; Kang, X.; Cui, Y. *Inorg. Chem.* **2018**, *57*, 9786. (c) Li, J.; Ren, Y.; Qi, C.; Jiang, H. *Chem. Commun.* **2017**, *53*, 8223.

(7) (a) Zeng, X.-P.; Sun, J.-C.; Liu, C.; Ji, C.-B.; Peng, Y.-Y. *Adv. Synth. Catal.* **2019**, *361*, 3281. (b) Kurono, N.; Ohkuma, T. *ACS Catal.* **2016**, *6*, 989. (c) Wang, W.; Liu, X.; Lin, L.; Feng, X. *Eur. J. Org. Chem.* **2010**, *25*, 4751. (d) North, M.; Usanov, D. L.; Young, C. *Chem. Rev.* **2008**, *108*, 5146. (e) Wingstrand, E.; Lundgren, S.; Penhoat, M.; Moberg, C. *Pure Appl. Chem.* **2006**, *78*, 409. (f) Brunel, J.-M.; Holmes, I. P. *Angew. Chem. Int. Ed.* **2004**, *43*, 2752. (g) Gregory, R. J. H. *Chem. Rev.* **1999**, *99*, 3649.

(8) Zhang, Z.; Bae, H. Y.; Guin, J.; Rabalakos, C.; van Gemmeren, M.; Leutzsch, M.; Klussmann, M.; List, B. *Nat. Commun.* **2016**, *7*, 12478.

(9) (a) Blackmond, D. G. *Angew. Chem. Int. Ed.* **2005**, *44*, 4302. (b) Mathew, J. S.; Klussmann, M.; Iwamura, H.; Valera, F.; Futran, A.; Emanuelsson, E. A. C.; Blackmond, D. G. *J. Org. Chem.* **2006**, *71*, 4711. (c) Zotova, N.; Broadbelt, L. J.; Armstrong, A.; Blackmond, D. G. *Bioorg. Med. Chem. Lett.* **2009**, *19*, 3934. (d) Mower, M. P.; Blackmond, D. G. *ACS Catal.* **2018**, *8*, 5977. (e) Dechert-Schmitt, A.-M.; Garnsey, M. R.; Wisniewska, H. M.; Murray, J. I.; Lee, T.; Kung, D. W.; Sach, N.; Blackmond, D. G. *ACS Catal.* **2019**, *9*, 4508. (f) Wei, B.; Sharland, J. C.; Lin, P.; Wilkerson-Hill, S. M.; Fullilove, F. A.; McKinnon, S.; Blackmond, D. G.; Davies, H. M. L. *ACS Catal.* **2020**, *10*, 1161.

(10) (a) Burés, J. *Angew. Chem. Int. Ed.* **2016**, *55*, 2028. (b) Burés, J. *Angew. Chem. Int. Ed.* **2016**, *55*, 16084. (c) Nielsen, C. D.-T.; Burés, J. *Chem. Sci.* **2019**, *10*, 348.

(11) (a) Maruyama, K.; Katagiri, T. *J. Phys. Org. Chem.* **1989**, *2*, 205. (b) Peltzer, R. M.; Gauss, J.; Eisenstein, O.; Cascella, M. *J. Am. Chem. Soc.* **2020**, *142*, 2984.

(12) Girard, C.; Kagan, H. B. *Angew. Chem. Int. Ed.* **1998**, *37*, 2922.

(13) Zhang, Z.; Klussmann, M.; List, B. *ChemRxiv* **2020**, preprintDOI: 10.26434/chemrxiv.12084768.v1.